Lawrence Berkeley National Laboratory

Title
DIRECT SURFACE STRUCTURE DETERMINATION WITH PHOTOELECTRON DIFFRACTION

Permalink
https://escholarship.org/uc/item/6zj031v1

Author
Barton, J. J.

Publication Date
1983

Lawrence Berkeley Laboratory

UNIVERSITY OF CALIFORNIA

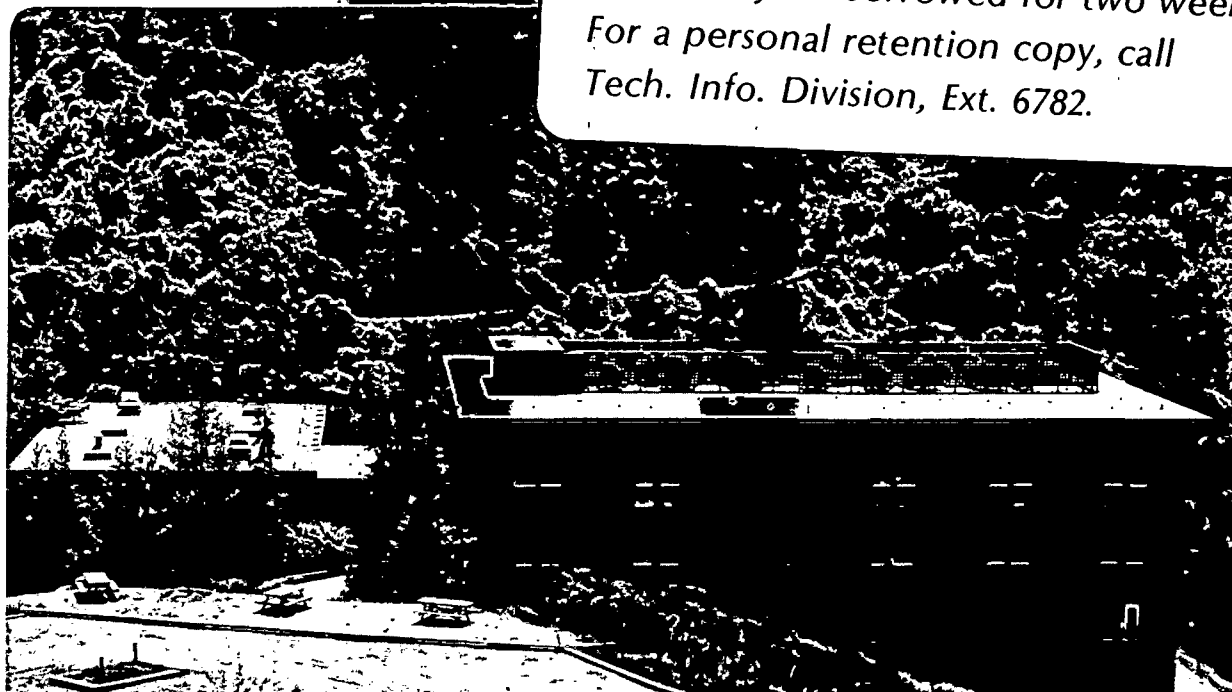## Materials & Molecular Research Division

DIRECT SURFACE STRUCTURE DETERMINATION WITH
PHOTOELECTRON DIFFRACTION

J.J. Barton, C.C. Bahr, Z. Hussain, S.W. Robey,
J.G. Tobin, L.E. Klebanoff, and D.A. Shirley

January 1983

DISCLAIMER

LBL-14645

DIRECT SURFACE STRUCTURE DETERMINATION WITH PHOTOELECTRON DIFFRACTION

J.J. Barton, C.C. Bahr, Z. Hussain*, S.W. Robey,
J.G. Tobin, L.E. Klebanoff, and D.A. Shirley

Materials and Molecular Research Division
Lawrence Berkeley Laboratory
and
Departments of Chemistry and Physics
University of California
Berkeley, California 94720

January 1983

*Present Address: University of Petroleum and Minerals, Dhahran, Saudi
Arabia.

ABSTRACT

Auto-regressive Fourier analysis of angle-resolved photoemission extended fine structure (ARPEFS) from adsorbate core levels yields complete, accurate surface structures. Scattering peaks from individual substrate atoms were observed using S(1s) photoemission from c(2x2)S/Ni(001) and p(2x2)S/Cu(001), along [011]. Fourfold-hollow site geometries were found for both systems, with interatomic distances of R(S-Ni) = 2.24(3) Å and R(S-Cu) = 2.28(3) Å.

In this Letter we show that photoelectron diffraction data, in the form of angle resolved photoemission extended fine structure (ARPEFS) from adsorbate core levels, can be transformed to give path length differences between primary and substrate-atom-scattered photoelectron waves. Analysis of these path length differences yields both distances and directions to nearby substrate atoms. For a given system, ARPEFS curves for one or more directions will thus provide a complete surface structure determination.

Energy-dependent photoelectron diffraction[1,2] has been used to determine adsorbate-substrate geometries for a number of systems.[3] Experimentally, photoemission into a selected angle is measured while the photoelectron kinetic energy is swept by varying a tunable photon source. Until now, analysis of the intensity variations with energy has been limited to trial-and-error comparisons with the results of scattering calculations.[4] Recently, normal emission theoretical curves over extended energy ranges,[5] and experimental curves over short ranges,[6] were Fourier-analyzed to yield peaks at distances close to adsorbate-substrate interplanar spacings, but the role of scattering phase shifts and the utility of this approach remained unclear.

Direct analysis begins by deriving the ARPEFS curve from the photoemission measurements. The intensity modulations, $\chi(h\nu)$, are extracted by removing the smooth atomic cross section: $\chi(h\nu) = (I-I_0)/I_0$, where I is the measured intensity and I_0 is the atomic cross-section. Then the Einstein and DeBroglie relations are

used to convert from photon energy to electron wave vector, $k = [2m(h\nu-E_0)/\hbar^2]^{1/2}$, where E_0 is an adjusted core-level binding energy. A single-scattering model[7] for photoelectron diffraction predicts the resulting ARPEFS modulations according to

$$\chi(k) = \sum_j \frac{\cos \beta_j}{\cos \gamma} \frac{|f(\alpha_j)|}{r_j} \cos[kr_j(1-\cos \alpha_j) + \phi_j], \qquad (1)$$

where the photoelectron wave encounters an ion core at a distance r_j from the source atom, scatters through an angle α_j with amplitude $|f(\alpha_j)|$ and, after a phase shift ϕ_j, propagates towards the detector. The angle between the polarization direction and the direct emission path is γ; the angle between the polarization direction and the initial path of an electron scattered from site j is β_j. Figure 1 illustrates the scattering geometry.

Eq. (1) suggests that a rather large number of path-length differences $\Delta R_j = r_j(1-\cos \alpha_j)$ can contribute to $\chi(k)$. However, two factors combine to emphasize the contributions from scatterers lying more or less directly behind the source atom (i.e., α_j near 180°). First, as Orders and Fadley[8] noted, $f(\alpha_j)$ tends to peak strongly near $\alpha_j = 0°$ and 180°, for electrons in the ARPEFS energy range of 100-400 eV. Second, the ($\cos \beta_j/\cos \gamma$) factor in Eq. (1) suppresses scattering from atoms at angles near 90° when the polarization direction is pointed into the detector.

The strong peaking in scattering amplitude near $\alpha_j = 180°$ suggests that alignment of the detector, an adsorbate atom, and a

substrate atom along the polarization direction would yield large ARPEFS modulations with a frequency near $2r_j$, i.e., twice the bond distance. Figure 2 shows the results of two such experiments for S(1s) photoemission along [011] in the overlayer systems c(2x2)S/Ni(001) and p(2x2)S/Cu(001), which were prepared by standard techniques[6,9]. Curves 2a and 2b both show large oscillations, and both contain the same dominant frequency. Since several reports[6,10] agree that S bonds in the fourfold hollow site on Ni(001), we may immediately conclude that S bonds in this same site on Cu(001). The energy range spanned by the S/Ni curve corresponds to a wave number range in $Å^{-1}$ of approximately one period (2π): the presence of four major oscillations thus indicates a path length difference ΔR of ~ 4 Å.

The ARPEFS data in Fig. 2 were analyzed by an auto-regressive linear prediction procedure,[11] followed by Fourier analysis, yielding the curves shown in Fig. 3. The excellent resolution is a consequence of the auto-regression step. The first three peaks in the middle curve of Fig. 3, at ΔR values of 2.0 Å, 3.5 Å, and 4.4 Å, all arise from the four nearest-neighbor nickel atoms along [110], lying respectively in front of, beside (2 Ni atoms), and almost directly behind the sulfur atom. The general form of these peaks establishes without further analysis that sulfur lies in a fourfold hollow site 1.3-1.4 Å above the surface, in agreement with the known structure.[6,10]. This curve alone approaches being a complete, self-contained structure determination, because these three peaks carry information about interatomic distances and directions to each

nearest neighbor Ni atom separately. Because scattering phase shifts[12] are known most reliably at present for backscattering through 180°, full analysis by back transformation[13] was applied to the ΔR = 4.42 Å peak alone. We derive R(S-Ni) = 2.24(3) Å, in excellent agreement with the result of Brennan, et al.[10]

A similar analysis on the "unknown" system p(2x2)S/Cu(001) yields similar results: a fourfold hollow site with ΔR = 4.54 Å, and R(S-Cu) = 2.28(3) Å (Figs. 2a and 3a). The structure of p(2x2)S/Cu(001) is thus determined.

Comparing the S/Ni and S/Cu Fourier transforms reveals another important ARPEFS feature: the intensities of peaks corresponding to atoms with $\beta_j \sim 90°$ will be strongly dependent on the polarization direction. The S/Ni measurements were made with the polarization vector aligned along the emission vector. The nearest neighbor with the shortest path length had $\cos \beta_j/\cos \gamma$ = 0.12. For S/Cu we tipped the polarization vector 15° closer to the surface, increasing the photoemission flux onto this atom--and hence the size of the first peak--by a factor of 5: $\cos \beta_j/\cos \gamma$ = 0.63. This polarization dependence provides a sensitive means for determining the exact angular position of individual substrate atoms.

Our results also provide a useful comparison of the ARPEFS and surface extended x-ray absorption fine structure (SEXAFS) techniques[14]. Figures 2c and 3c reproduce the SEXAFS modulations and Fourier transform reported by Brennan et al[10]. SEXAFS is an angle integrated measurement of the absorption cross section. Its

modulations vary as $\sin(2kr + \phi_b + \phi_a)$, oscillating with a frequency close to twice the bond length. ARPEFS is an angle-resolved measurement following $\cos(kr_j(1-\cos \alpha_j) + \phi_j)$. The frequency evident in Figs. 2a and 2b is close to twice the bond length because the modulations are dominated by scattering from the nearest neighbor directly behind the sulfur. SEXAFS has both an absorber and a backscatterer phase shift; ARPEFS has only a backscatterer shift. The SEXAFS modulations are ± 2%; the ARPEFS modulations are larger by $kr_j \sim 10$. The SEXAFS polarization dependence has the form of an intensity $(\cos^2 \beta_j)$; the ARPEFS polarization dependence follows an amplitude $(\cos \beta_j)$. But Fig. 3 illustrates the most important difference: each near neighbor appears as a separate peak in the ARPEFS Fourier transform. The positions and intensities of these peaks carry information about the distances and directions of neighboring atoms and they can be varied by adjusting the emission and polarization vectors.

In summary, we have reported experimental evidence for the dominance of single backscattering in photoelectron diffraction. The use of ARPEFS directly to solve the p(2x2)S/Cu(001) structure demonstrates its power as a probe for surface structures. With the increasing performance of synchrotron radiation facilities, wide energy-range photoemission data can be obtained for all elements, including the technologically and biologically important low Z elements. The angle-resolved nature of ARPEFS gives it promise for the study of molecular and multi-site atomic adsorbates. Disputed

surface structures may be determined unambiguously by placing an angle-resolved detector opposite an expected substrate atom and recording the resultant ARPEFS. Complicated adsorbate systems can be analyzed along a variety of emission axes. By careful choices and variation of emission and polarization directions, it may even be feasible to determine bond angles to within 1-2°.
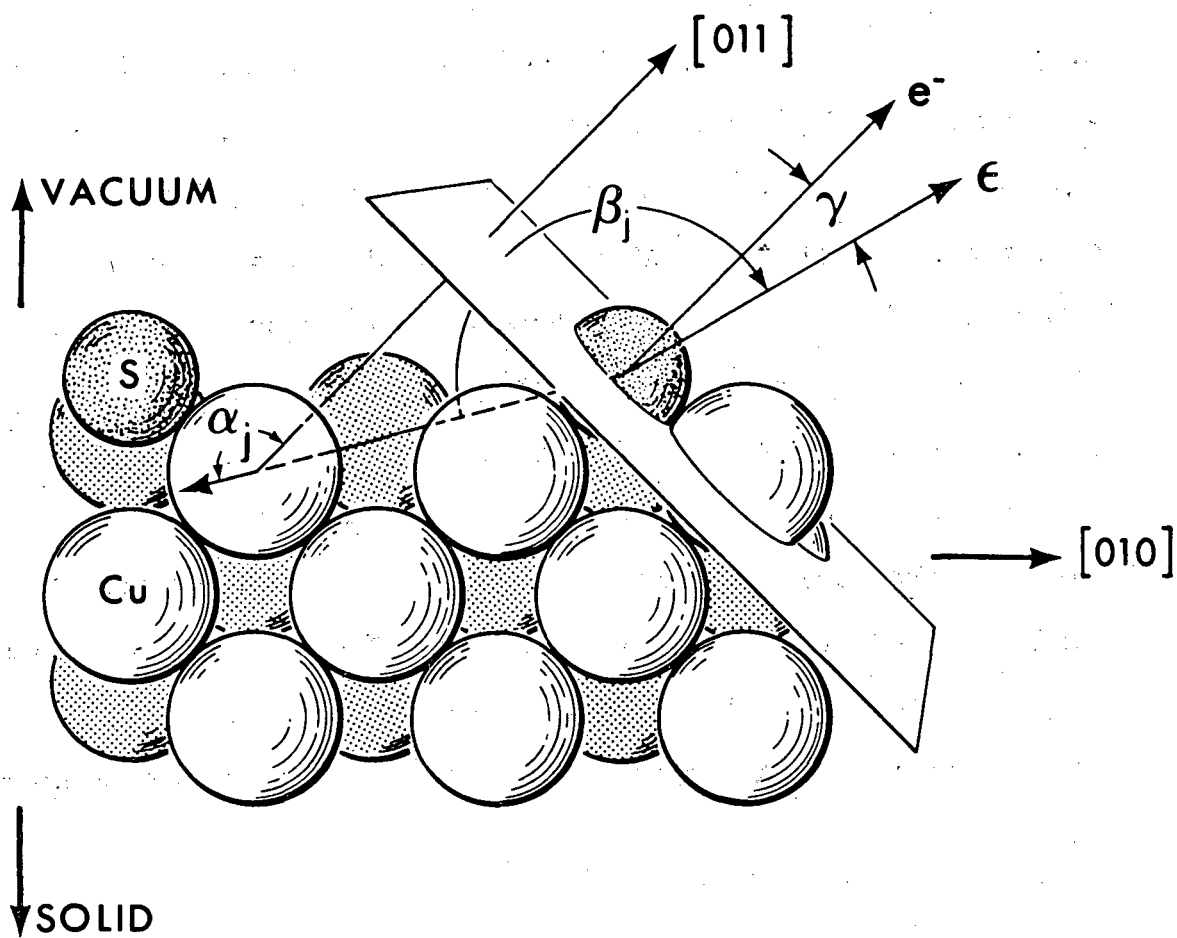
Acknowledgements

References

1. A.Liebsch, Phys. Rev. Lett. 32, 1203 (1974).

2. S.D.Kevan, D.H.Rosenblatt, D.R.Denley, B.-C.Lu, and D.A.Shirley, Phys. Rev. Lett. 41, 1565(1978).

3. S.Y.Tong and C.H.Li, Critical Reviews of Solid State Sciences 10, 209, CRC Press, 1981.

4. S.Y.Tong, C.H.Li, and A.R.Lubinsky, Phys. Rev. Lett. 39, 498 (1977); C.H.Li, A.R.Lubinsky, and S.Y.Tong, Phys Rev. B 17, 3128(1978).

5. Z.Hussain, D.A.Shirley, C.H.Li, and S.Y.Tong, Proc. Natl. Acad. Sci. USA 78, 5293(1981).

6. D.H.Rosenblatt, J.G.Tobin, M.G.Mason, R.F.Davis, S.D.Kevan, D.A.Shirley, C.H.Li, and S.Y.Tong, Phys. Rev. B 23, 3828(1981).

7. Derived by analogy with P.A.Lee and J.B.Pendry, Phys. Rev. B 11, 2795(1975). A similar formula from T. Fujikawa, J. Elect.Spect. 22, 353(1981) differs in sign.

8. P. Orders and C. Fadley, submitted to Phys. Rev. B.

9. The overlayer was prepared by exposing clean Cu(001) to ~75 x 10^{-6} torr-sec $H_2S_{(g)}$ and heating the crystal to ~ 500K. The p(2x2) structure was confirmed by in-situ LEED.

10. S.Brennan, J.Stöhr, and R.Jaeger, Phys. Rev. B 24, 4871(1981).

11. J.J.Barton and D.A.Shirley, to be published.

12. P.A.Lee, B.K.Teo, and A.L.Simons, JACS 99, 3856(1977).

13. G.Martens, P.Rabe, N.Schwenter, and A.Werner, Phys. Rev. B 17, 1481(1978).

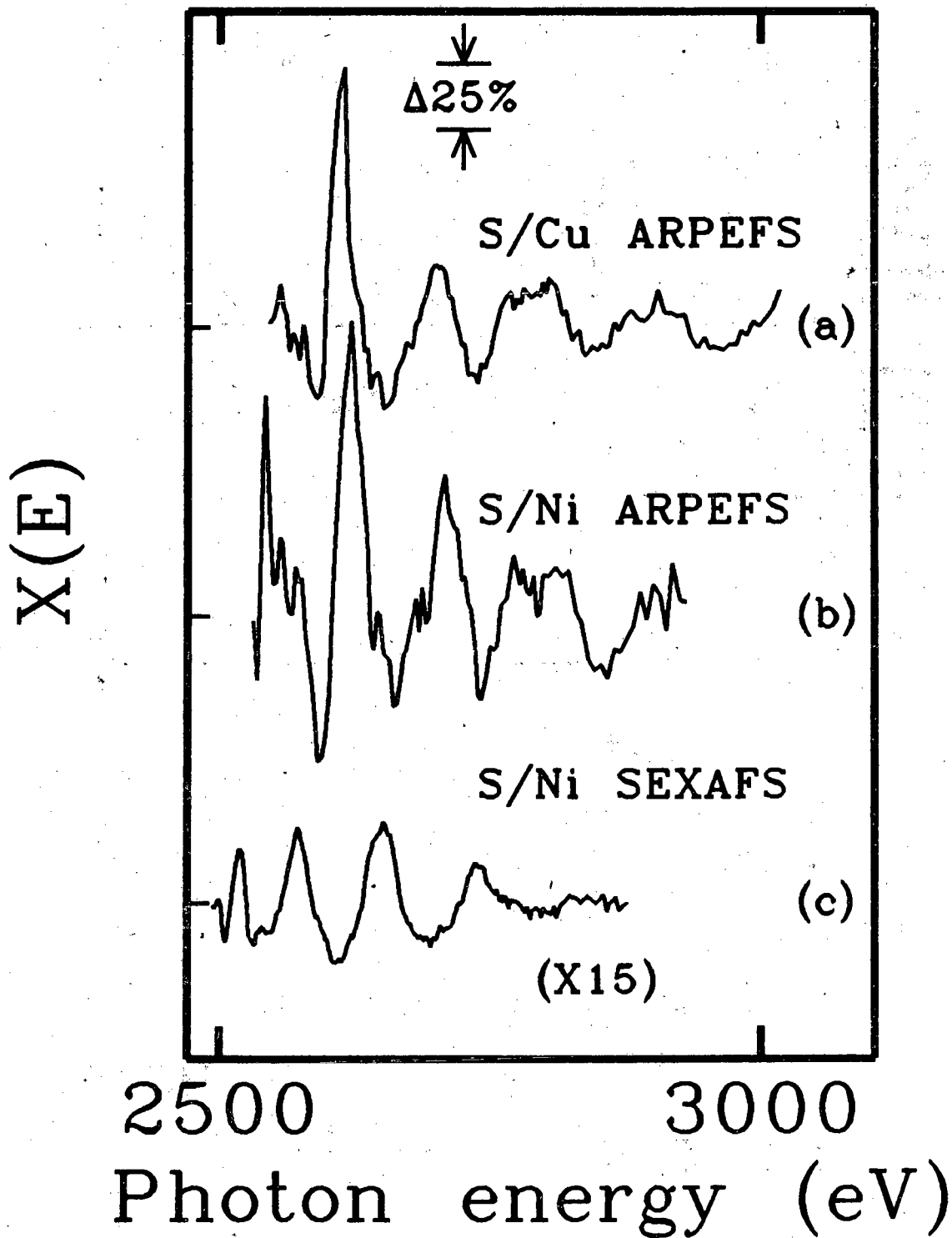14. P.A.Lee, Phys. Rev. B 13, 5261(1976).

Figure captions

1. Cross-sectional view of a fcc crystal (001) surface showing the experimental geometry and illustrating the parameters of the analytic single scattering formula. The angle resolved detector is along the vector labeled e^-([011] direction); the polarization vector is ε. The angle between these two vectors is γ. The vector from the emitter to the scattering atom j makes an angle β_j with the polarization vector and an angle α_j with the emission direction.

2. $\chi(E)$ curves are shown for (a) p(2x2)S/Cu(001) ARPEFS in the [011] direction, (b) c(2x2)S/Ni(001) ARPES in the [011] direction, and (c) c(2x2)S/Ni(001) SEXAFS of Brennan et al., ref. 10.

3. Comparison of Fourier transform amplitudes for (a) ARPEFS from p(2x2)S/Cu(001), (b) ARPEFS from c(2x2)S/Ni(001), and (c) SEXAFS from c(2X2)S/Ni(001) from ref. 10. The ARPEFS range in k-space was extended using the auto-regressive estimation method prior to Fourier transformation.
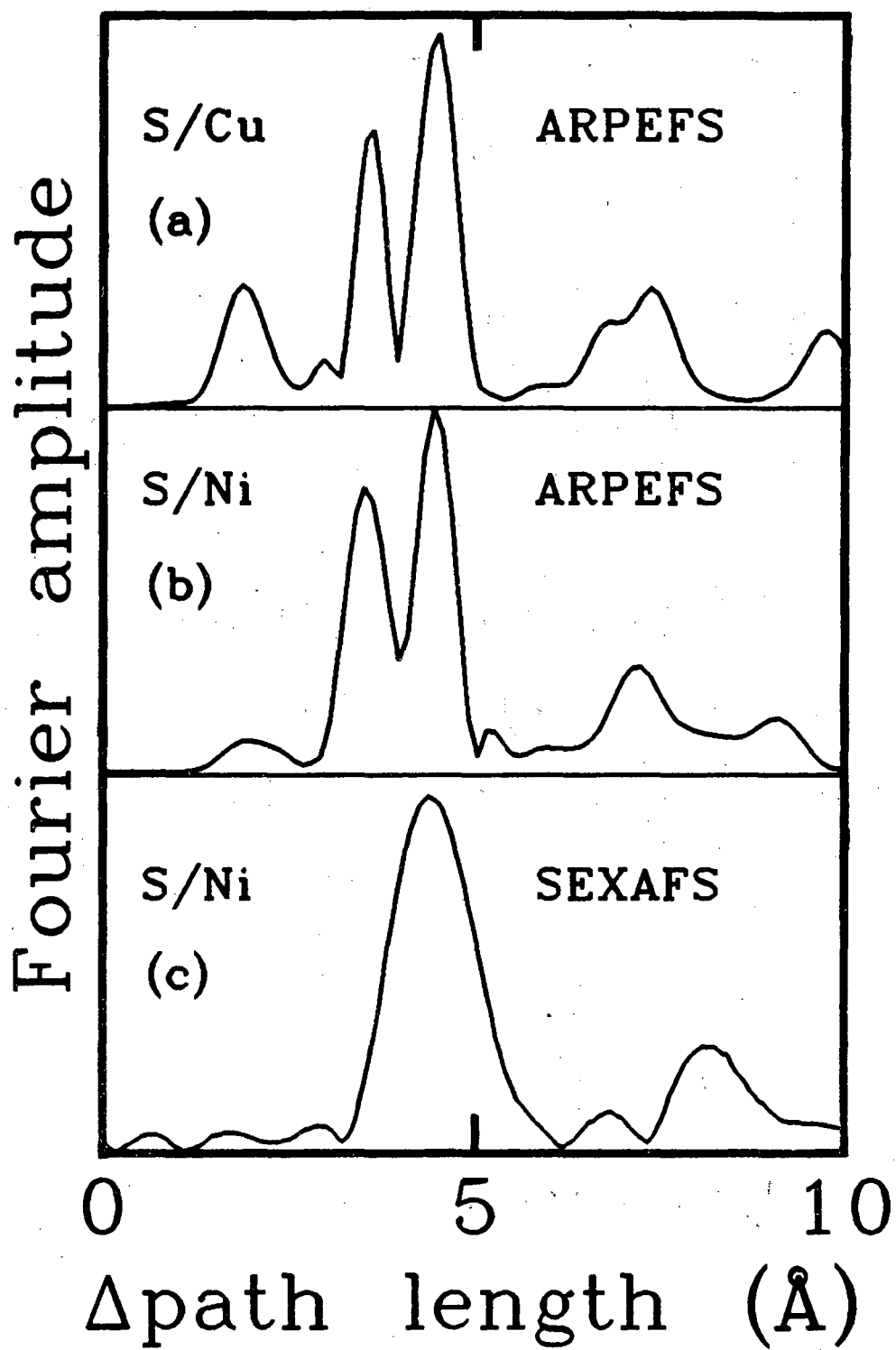
p (2x2) S/Cu(001)

XBL 8212-7380

Figure 1

Figure 2

XBL 8212-12282

Figure 3